NCI Workshop on Proton Therapy for Children: Considerations Regarding Brainstem Injury

Daphne Haas-Kogan, M.D.,

Department of Radiation Oncology, Harvard Medical School and Brigham and Women's Hospital, Dana-Farber Cancer Institute, Boston Children's Hospital, Boston

Daniel Indelicato, M.D.,

Department of Radiation Oncology, U of Florida, Jacksonville, FL

Harald Paganetti, M.D.,

Department of Radiation Oncology, Harvard Medical School and Brigham and Women's Hospital, Dana-Farber Cancer Institute, Boston Children's Hospital, Boston

Natia Esiashvili, M.D.,

Radiation Oncology Department, Winship Cancer Institute, Emory University, Atlanta

Anita Mahajan, M.D.,

Departments of Radiation Oncology, M D Anderson Cancer Center, Houston, and Mayo Clinic, Rochester, MN

Torunn Yock, M.D.,

Department of Radiation Oncology, Harvard Medical School and Massachusetts General Hospital, Boston

Stella Flampouri, Ph.D.,

Department of Radiation Oncology, U of Florida, Jacksonville, FL

Shannon MacDonald, M.D.,

Department of Radiation Oncolgy, Harvard Medical School and Massachusetts General Hospital, Boston

Maryam Fouladi, M.D.,

Cincinnati Children's Hospital Medical Center, Cincinnati

Stephen Kry, Ph.D.,

UT M D Anderson Cancer Center, Houston

John Kalapurakal, M.D.,

Department of Radiation Oncology, Northwestern Memorial Hospital, Chicago

Stephanie Terezakis, M.D.,

Corresponding Author: Larry E. Kun, M.D., Department of Radiation Oncology, UT-Southwestern Medical Center, 2280 Inwood Road, Dallas, TX 75390; larry.kun@utsouthwestern.edu; 214-645-7683.

Department of Radiation Oncology, Johns Hopkins Medical Institute, Baltimore

Hanne Kooy, Ph.D.,
Department of Radiation Oncology, Harvard Medical School and Massachusetts General Hospital, Boston

David Grosshans, M.D., Ph.D,
UT M D Anderson Cancer Center, Houston

Mike Makrigiorgos, Ph.D.,
Department of Radiation Oncology, Harvard Medical School and Dana-Farber Cancer Institute, Boston

Kavita Mishra, M.D., M.P.H.,
Department of Radiation Oncology, University of California at San Francisco

Tina Young Poussaint, M.D.,
Department of Radiology, Harvard Medical School and Dana-Farber Cancer Institute, Boston Children's Hospital, Boston

Kenneth Cohen, M.D.,
Johns Hopkins University/Sidney Kimmel Cancer Center

Thomas Fitzgerald, M.D.,
UMass Memorial Medical Center, Massachusetts

Vinai Gondi, M.D.,
Northwestern Medicine Chicago Proton Center, Chicago

Arthur Liu, M.D.,
University of Colorado School of Medicine, Aurora

Jeff Michalski, M.D.,
Washington University St. Louis School of Medicine, St. Louis

Dragan Mirkovic, Ph.D,
UT M D Anderson Cancer Center, Houston

Radhe Mohan, Ph.D,
UT M D Anderson Cancer Center, Houston

Stephanie Perkins, M.D., Ph.D.,
Washington University St. Louis School of Medicine, St. Louis

Kenneth Wong, M.D.,
Children's Hospital of Angeles and University of Southern California Keck School of Medicine

Bhadrasain Vikram, M.D.,
Radiation Research Program, National Cancer Institute, NIH, Rockville, MD

Jeff Buchsbaum, M.D., and
Radiation Research Program, National Cancer Institute, NIH, Rockville, MD

Larry Kun, M.D.

Department of Radiation Oncology, UT-Southwestern Medical School, Dallas

Radiation therapy is an important component of the multimodal approach to cancer treatment. There has been continual, significant improvement in both photon and proton radiation therapy with more precise dose conformality.[1] Advances in technology aim to improve outcomes, including disease control and quality of life, the latter through reduction in untoward effects.[2] Proton therapy can significantly reduce radiation dose to critical normal tissues, important to preserving functional capabilities.[3–5] By reducing the unintended medium and low radiation doses in normal tissue structures, proton therapy can potentially reduce both short-term and long-term deleterious radiation effects.[5]

The proton beam model policy adopted by the American Society of Radiation Oncology (ASTRO) in 2017 supports proton therapy in primary solid neoplasms in children treated with curative intent.[6] Proton beam radiation is particularly appealing in treating primary brain tumors in children. The number of pediatric patients treated with proton therapy continues to increase significantly,[5, 7] and proton therapy is now an option for many Children's Oncology Group (COG) protocols.

As more children have been treated with protons, there is a growing body of literature that suggests possible lower rates of treatment-related morbidities,[8–14] including cognitive effects[15–19] and secondary malignancies,[20–23] as well as physical and psychosocial domains impacting quality of life.[24] At the same time, there have been reports of uncommon but significant morbidities, including brainstem injury in the setting of posterior fossa tumors treated with proton beam radiation.[7, 25–28] Two recent commentaries summarized concerns regarding brainstem necrosis in children following proton therapy, while highlighting the limited data indicating this rare event may be more common following proton irradiation.[29, 30] The NCI convened a *Workshop on Proton Therapy for Children: Caveats and Opportunities* in May 2016 to examine brainstem injury in children following proton therapy. This paper summarizes the data and interpretations presented at the Workshop that included 27 participants: radiation oncologists expert in pediataric brain tumors, radiation physicists with expertise in proton beam irradiation, and experienced investigators in radiation biology, neuroradiology, pediatric neuro-oncology, and research administration from NCI.

The current report describes our understanding of the clinical extent of brainstem injury following proton therapy and factors that may correlate with clinical and neuroimaging signs. We consider the influence of radiation therapy parameters on brainstem injury, including target and normal structure definitions and expansions, target volume dose, brainstem dose constraints, and treatment planning and delivery approaches. Unlike photons, use of protons also raises questions of differences in linear energy transfer (LET) and relative biologic effect (RBE) that are known to differ within the distal segments of the spread out Bragg peak (SOBP). Standard RBE correction of physical dose for protons is uniformly applied, raising uncertainties for proton delivery in posterior fossa tumors, especially with plans that include one or more beams that deposit dose toward the end of the SOBP in the brainstem. The importance of differences in both LET and RBE and the low α/β ratio of brain tissue are more apparent as treatments move from scatter beam, collimator

defined proton therapy toward intensity modulated proton therapy (IMPT) and pencil beam techniques that may further modify the LET and RBE.[31, 32] The data reviewed at the Workshop and herein reported address experience solely with scatter and uniform active scanned beam therapy.

The Workshop summary considers clinical phenomena in the context of similarities and differences in proton treatment parameters among three institutions that were asked to report their clinical data on the treatment of large numbers of children over the prior 10 years.

Clinical Experience

The three largest U.S. pediatric proton therapy programs independently analyzed their data regarding post-irradiation brainstem toxicity in children with posterior fossa tumors who were treated according to institutional guidelines. The centers (Massachusetts General Hospital - MGH, M D Anderson Cancer Center - MDA, University of Florida - UF) have institutional review board approved studies to retrospectively evaluate their experience and have applied uniform inclusion criteria and toxicity grading using a modified CTCAE v4.0 scale [7].

All patients   21 years old treated with focal proton therapy alone for posterior fossa tumors were analyzed except those with intrinsic brainstem tumors (i.e., diffusely infiltrating brainstem gliomas or other primary intra-axial brainstem tumors) and those who had received prior irradiation to the brain or skull base. To minimize variability in treatment delivery, patients were not included if their therapy included a photon component that exceeded 5% of dose or fractionation other than 1.8 Gy once daily. Any patient with insufficient follow-up (< 6 weeks from completion of irradiation or lack of follow-up MRI) was excluded. Brainstem toxicity was defined according to Indelicato [7] as: (a) new or progressive symptoms and/or signs following irradiation involving motor weakness or cranial nerves V–VII or IX–XII, (b) corresponding radiographic abnormalities within the brainstem, and (c) absence of local disease progression.

The collective experience from the three centers included 671 children with posterior fossa tumors treated with proton therapy between 2006 and 2016. Fifty-seven percent of the patients had medulloblastoma; 29% had ependymoma. The remaining 14% had gliomas and atypical teratoid rhabdoid tumors. The median patient age was 5.4 years (range 0.5–21.8). The median follow-up for patients at each center was 3 years (range 0.1–14.7). Consistent with published data from other large single-institution proton series,[1, 26, 33–35] the average rate of grade 2+ (symptomatic) brainstem toxicity was 2.38%. The average rate of grade 3+ brainstem injury was 1.3%, and that of fatal brainstem injury, 0.4%. Toxicity was primarily managed with high dose steroids.

Results from Emory Winship Institute following *photon* IMRT therapy were presented and later published [38]. This analysis involved 60 contemporary patients with posterior fossa tumors and applied similar inclusion criteria. The prescription dose and tumor histology distributions were similar to the experience at the 3 proton centers. The median follow-up was slightly less at 2.8 years (range 0.1–4.8). This cohort was similar to the proton datasets

in that median age was 6.7 years (range 1.4–21.8), and 27% of the patients carried the diagnosis of ependymoma. When symptoms of brainstem injury were combined with radiographic correlates as defined by Indelicato, [7] brainstem toxicity was observed in 6.7%. The rate of grade 3+ brainstem toxicity was 3.3%, consistent with published toxicity rates from other large single-institution photon series involving posterior fossa tumors.[26, 36, 37] The rate of fatal brainstem toxicity was 1.7%. The data compare to published experience from St. Jude Children's Research Hospital reporting 4.4% incidence of symptomatic brainstem injury following photon therapy for infratentorial embryonal tumors and 2.5% with infratentorial ependymomas.[37, 38]

Across all centers and radiation modalities (protons and photons), patients with brainstem necrosis were more likely to have received higher prescription doses and higher doses to the brainstem. Patients with brainstem necrosis had an average prescription dose of 55.7 Gy, with D50, D10, and DMax of 54.7 Gy, 56.8 Gy, and 58.0 Gy, respectively. Patients without brainstem necrosis had an average prescription dose of 54.6 Gy, with D50, D10, and DMax of 51.7 Gy, 55 Gy, and 56 Gy, respectively. The suggestion of dose-effect is consistent with published data from both photon and proton series.[39]

A dose effect is apparent in a recent analysis by Indelicato et al. that summarizes the University of Florida experience with proton irradiation for posterior fossa ependymomas between 2007 and 2017.[40] Outcomes in 63 patients treated according to Children's Oncology Group (COG) ACNS0831 (trial for newly diagnosed ependymomas) radiation guidelines for brainstem dose (D50<61 Gy, D10<63 Gy – goal; maximal D50<62 Gy and D10<64 Gy) were compared to 56 patients treated on modified guidelines incorporating age (greater or less than 5 years old) and 3 dose-volume benchmarks (see Table 1 for details). Rates of local disease control, progression-free survival, and overall survival at 3 years did not differ between the 2 cohorts, while the actuarial rate of grade 2+ brainstem toxicity at 1.5 years was 12.7% in children less than 5 years old in the earlier cohort and zero in those treated using the modified guidelines.

COG has responded to concerns regarding brainstem injury following proton irradiation by proposing modifications for the ongoing ependymoma clinical trial (ACNS0831). In the previous COG ependymoma trial (ACNS0121), brainstem necrosis was reported in 2 of 324 children following photon therapy and 2 of 20 after proton therapy. Of the two cited cases among the 20 proton patients, there was a single case of grade 1 necrosis (asymptomatic; clinical or diagnostic observations only; intervention not indicated) and a single case of grade 2 necrosis (moderate symptoms; corticosteroids indicated). The data are not definitive, as they lack site-specific information, consistent review of post-irradiation imaging, and an agreed upon threshold for *symptomatic* brainstem injury (i.e., CNS grade 2+); furthermore, the proton beam radiation cohort is limited in size. A revision is proposed to the radiation guidelines for ACNS0831 reducing the CTV volume expansion and brainstem tolerance doses. The changes include limiting the initial clinical target volume (CTV) expansion to 3 mm depth within the brainstem for both photons and protons and an obligatory reduction in CTV after 54 Gy. The proposed quantitative normal tissue constraints for photons and protons for the brainstem are as follows: 1) Goal: Brainstem D50 61 Gy and D10 63 Gy (photons) vs. D50 52.4 Gy and D0.1 cc 56.6 Gy (protons); 2) Maximum: Brainstem D50

62 Gy and D10 64 Gy (photons) vs. D50 54 Gy and D0.1cc 58 Gy (protons). There have been no reports of grade 4 CNS toxicity on COG ACNS0831; the study is ongoing. (personal communication, Children's Oncology Group, December 2016)

Imaging Findings of Brainstem Injury

MR imaging is central to documentation of post-irradiation brain injury.[28, 41–45] Imaging signs of CNS injury include: focal or diffuse T2 prolongation on FLAIR images, areas of contrast enhancement on gadolinium-enhanced T1 sequences, focal areas of intra-axial hemorrhage, and signs of encephalomalacia and frank necrosis.[7, 26, 46] Imaging findings in the brainstem are outside the primary tumor site are usually signs of injury.[7, 41, 47] All patients reviewed for this paper had primary tumors that did not involve the substance of the brainstem, while symptomatic radiation-induced lesions specifically within the brainstem are the critical toxicity of interest reported herein.

In evaluating intrinsic brainstem findings, changes in diffusion tensor imaging [DTI] have been correlated with demyelination secondary to irradiation.[43] Serial DTI measures following incidental brainstem irradiation show alterations in fractional anisotropy [FA] and diffusivity.[41, 47] Reduction in FA is often seen during the first year post-irradiation absent symptomatology; imaging abnormalities may be isolated or may precede clinical symptoms or signs, often by several months..[38, 41]

Correlations of LET with dose and imaging have been reported, matching *in vivo* anatomy of the posterior fossa and post-irradiation changes within the brainstem to tract-averaged LET, showing apparently lower physical doses associated with imaging changes in areas of higher LET.[48] The methodology has yet to be validated. There has been no evidence of unique neuroimaging findings related to protons or heavy ions.

LET and RBE

The relative biological effectiveness (RBE) value of 1.1 that is the basis for today's clinical practice with proton beam radiation therapy is based on *in vitro* cell survival data obtained at the center of an SOBP, as well as animal studies done in the early 1970's.[49] RBE is defined as the ratio of doses required to achieve the same biological effectiveness between different treatment modalities. RBE depends on dose and on biological endpoints (or α/β if characterized by the linear-quadratic dose-response relationship). There appears to be a trend towards an increase in RBE as α/β or dose per fraction decrease [50].

In addition to dose and α/β, RBE depends on the linear energy transfer (LET). The key to understanding radiation effects lies in the spatial distribution of energy deposition events and the complex radiation-induced lesions this may cause. The distribution of double-strand breaks caused by different types of irradiation can vary significantly depending on the energy deposition patterns of the incident photon or proton. Damage from protons can be more complex than that from photons [51]. The LET is the average amount of energy that radiations impart to the local medium per unit length. It affects the type of damage but also the capacity of the cell to repair the damage [52]. LET is an approximation of a particle's ionization track structure, which determines the physics characteristics of a radiation field.

Proton energy decreases as a function of depth in the Bragg curve, which causes an increase in LET in a pristine peak as well as in a SOBP. Using a model based on average values of all published data [53], assuming α/β=3 Gy, 1.8 Gy per fraction and for a typical SOBP delivery, the RBE relative to 6 mV photons for *in vitro* cell survival increases with depth from ~1.1 in the entrance region, to ~1.15 in the center, ~1.37 at the distal edge and ~1.74 in the distal fall-off (assuming dose averaged LET values of 1, 2, 7, and 16.6 keV/μm). Note that the value in the center of the SOBP, 1.15, is slightly higher than 1.1, which is in line with the goal to define RBE conservatively in terms of tumor control and thus conversely aggressively in terms of organ at risk dose. The available experimental data can be used to create an empirical RBE model for cell survival.

Although there is a large amount of data on the RBE for clinically relevant LET values, tissue α/β values, and doses, the proton RBE is still associated with considerable uncertainties that would lead to broad error bars in RBE weighted dose-volume histograms [54]. The above values are average for RBE and may deviate significantly in human tumors *in vivo*. In addition, while cell survival might be the most relevant effect for tumor control probability (TCP) considerations, other endpoints could potentially be more relevant for early and late normal tissue complication probability (NTCP). Thus, conclusions about an average RBE for organs at risk cannot be based on clonogenic cell survival and thus, treatment planning based on local RBE variations seems premature at this point. It is questionable whether available models and their incorporation into the treatment planning process would result in better clinical outcomes. Furthermore, as PTV contours include tumor as well as healthy tissues, there could be differences in α/β for the same volume that could lead to unanticipated variations in the DVH that would be difficult to interpret.

Evaluation of empirical LET-sparing versus dose-sparing techniques for normal tissues

In proton therapy, the elevated LET values at the end of range and the associated increase in RBE are of concern, especially when the distal end of a treatment field is directed towards a sensitive structure. This report focuses on the treatment of posterior fossa tumors where at least partial inclusion of the brainstem in the target is necessary, and the optimal beam geometry for tumor coverage and dose conformality often directs the SOBP distal edge towards this critical structure. Since the clinical use of LET or RBE distributions in treatment planning are still not established, current centers apply brainstem-sparing planning and delivery techniques. In these techniques, the physical dose is carefully conformed to the target volume, allowing the distal end of only one beam to be placed within the brainstem and constraining the maximum physical dose to this sensitive structure.[55]

LET versus RBE based planning

While RBE values in tissues are not well known, LET is based on physical properties and can be calculated accurately based on treatment plan information [56]. Although LET does not uniquely determine actual proton RBE, it is an indicator for local increase or decrease of RBE. Amongst the published models there is a consensus that proton RBE increases in approximately linear fashion with LET over the range of LET values significant for proton therapy. Thus, while the absolute RBE for a given organ or tumor is not well known and is likely patient specific, the fact that RBE increases with LET within a given organ/tumor

seems undisputed with only the slope of the relationship being patient dependent. RBE based planning may not necessarily result in a better plan in terms of RBE-weighted dose because the RBE is not known precisely. It is also unclear how to set RBE-weighted dose constraints in the optimization. In contrast, LET based optimization is a simplified approach that tries to minimize LET in certain structures. In view of the observed general increase of RBE with LET, LET based optimization should result in a favorable plan for the structure of interest, if one also assumes constant physical doses independent of patient-specific factors.

LET based planning for normal tissues

The dose-averaged LET (LET_d) can be used in biological treatment optimization even without accurately knowing dose and specific RBE values for normal tissues [57]. In intensity-modulated proton therapy (IMPT), LET distributions can be shaped appropriately without altering the dose constraints in treatment planning; i.e., dosimetrically equivalent plans can show significant differences in LET distributions (Figure 1).

It has been demonstrated that by considering spatial variations in LET_d within treatment plan optimization, it is possible to increase the therapeutic ratio in IMPT [57, 58]. The strategy is to utilize the fact that the RBE increases with LET for a given dose and α/β and thus design an optimization algorithm that moves elevated LET regions away from certain areas/organs, e.g. tissues with low α/β [57, 59, 60].

LET-based optimization of IMPT plans represents a pragmatic approach to bridge the gap between purely physical dose-based and RBE-based planning [61]. The method makes IMPT treatments safer by mitigating a potentially increased risk of side effects due to elevated RBE of proton beams near the end of range. In this method, one first determines an IMPT plan based on physical dose objectives, as is current clinical practice. In a second step, the LET distribution is modified to avoid high LET values in critical structures. This strategy comes at a relatively small penalty (~2–3% in extra dose).

LET based optimization could be used, for instance, to reduce LET (and thus RBE) in the brainstem, without changing current planning strategies, dose constraints, prescription doses, and clinical plan assessments [61]. Treatment planning systems would have to add a second, LET based, optimization step.

LET based planning for the target

The goals above for normal tissues are achieved with the proposed combination of physical dose and LET-guided planning. Optimizing biological dose in the GTV has also been addressed by combining physical dose optimization with the goal of influencing the LET distribution [57, 60, 62, 63]. However, attempts to concentrate high LET exclusively in the GTV are typically associated with degradation of the physical dose distribution [61]. An alternative strategy is to allow higher physical dose in the GTV. Hence, to assess the potential benefit of LET escalation in the GTV, such treatment plans should be compared to what physical dose escalation can achieve. Higher doses in parts of the GTV can often be achieved without increasing normal tissue dose. Overall, it appears that LET based optimization holds more promise for healthy tissues than for tumors.

Future LET and RBE treatment planning work

LET based optimization allows biological treatment plan optimization without changing current prescription doses or dose constraints. This, in turn, offers the possibility of studying the methodology in safe clinical trials. Optimizing based on LET instead of RBE circumvents RBE uncertainties but only considers the physics parameters pertaining to RBE. With or without considering LET or RBE directly in the treatment planning optimization process, we should at least evaluate plans for LET robustness or, if dose-response relationships are reasonably well known for specific structures in the future, for RBE robustness.

To motivate RBE or LET based planning, clinical evidence needs to be presented to suggest such planning leads to improved outcomes. Evidence could come from early or late effects in regions of low α/β and/or high LET. This would occur, for example, if an SOBP field ranges out in the brainstem when treating targets in the brain. Toxicities (e.g. brainstem necrosis) found in 4 out of 111 (3.6%) medulloblastoma patients were recently analyzed [34]. No clear correlation between elevated LET and regions of toxicity was found although the sample size was relatively small. In a separate study on ependymoma patients, the authors indicate that they saw a clear correlation between areas of elevated LET and of radiographic changes in 14 children.[48] However, such early results might eventually become confounded by inter-patient biological variability and therapeutic intervention heterogeneity that might prove to be larger than RBE variations. Though there were some suggestions of increased risk of brainstem toxicity with the use of chemotherapy and/or surgery, no consistent relationshiop has been identified in these studies thus far.[7, 25–28] RBE based optimization may require precision medicine approaches be incorporated into radiation therapy treatment planning.[64]

Posterior Fossa Proton Radiation Therapy – Absolute dosimetry, Clinical Treatment Planning and Delivery

Absolute Dosimetry and isodose calculation

There is an important relationship between absolute dose and proton equipment monitor units (MUs). For SOBP fields, this relationship has been difficult to formalize, as compared to, for example, photon or proton pencil-beam dose calculations. One reason for the complexity of converting isodoses to absolute MU is the great variability of SOBP delivery systems. A change in any of the upstream proton components (aperture, range compensator or energy modulation devices) creates a separate "nozzle", i.e. a distinct proton beam with its own dependence on the MU. Accordingly, SOBP treatment planning software calculates only proton isodose lines, while the assignment of absolute number of MUs to fields is assigned externally via calibration.

Briefly, these are the steps followed at MGH for SOBP treatment planning and dosimetry:

   1.   The planner defines an SOBP field in terms of an aperture, range-compensator, distal range and proximal range. These all affect the dose in the patient.

2. The treatment planning system (or planner) assigns a value of 100% dose in water to the SOBP flat top in the absence of the aperture and range-compensator.

3. The effect of the aperture, range-compensator and patient produce a dose distribution through the target volume with some variability of dose around the nominal 100%. The planner ensures that the target minimum dose is 100% by applying a normalization factor F.

4. The planner assigns the field dose Df to this 100% isodose.

5. The physicist then establishes how many MU must be delivered in water to deliver an absolute dose Df to the flat top of the SOBP field. The specific MUf required to deliver the dose Df for this field are MU / F. There are three methods to derive MUf:

    a. Measure MUf of each individual field. This was the practice at the Harvard Cyclotron Laboratory – a major investment in manpower.

    b. Use a physical model to compute the MUf. This is described in Kooy, [65] and is the model used at both MGH and UF.

    c. Use an empirical model that establishes all the variables and measures a complement of MU as a function of these variables. This is described by Sahoo, [66] and is the practice at MDA.

6. Absolute calibration of the models used is performed in terms of physical dose (i.e. Gy) and is traceable to the national standard.

The algorithms to calculate isodoses for the patients under consideration use two models:

1. Varian Eclipse – Used at UF and MDA. (This model was developed by B. Schaffner at Varian.)

2. MGH (Astroid) – This is based on the model described in Hong, [67] and re-implemented by Madden & Kooy.

Either dose algorithm implementation should perform well in the geometry of the posterior fossa.

Additionally, the use of Monte Carlo provides a high level of redundancy to the relative and absolute dosimetry. Monte Carlo validation of isodoses calculated by the dose calculation algorithms is continually applied in all clinical cases at MGH.

Pre-treatment Work-up

The pre-treatment work-up for pediatric posterior fossa treatments is standardized for all three institutions:

1. Supine positioning on a base-of-skull board and a thermoplastic mask.

2. CT acquisition and reconstruction using 1–1.5 mm slices (through the target region and required, adjacent relevant normal structures)

3. Anesthesia and intubation when required

4. All relevant and appropriate MRI studies are registered to the treatment planning CT using rigid registration.

Treatment Planning and Delivery Considerations

The cohorts at the three institutions described in this paper were planned with SOBP fields; the text relates solely to its use. Target and OARs were delineated and peer-reviewed. Institutional-specific treatment planning details are outlined in Table 1. Of note, some of the depicted Figures also provide pencil beam scanning (PBS) examples for comparison to the SOBP cases on which the current paper is focused.

SOBP practice for the treatment of posterior fossa ependymoma has recently shifted for many instiutions to reducing the dose to the brainstem and, on occasion, also to the target volume, if indicated, to a total dose of 54.0 Gy (RBE). Thus, the University of Florida uses a prescription of 59.4 Gy (RBE) to the target but stops the full field, including the brainstem, at 54.0 Gy (RBE); the remaining 5.4 Gy (RBE) is delivered with fields that avoid the brainstem (Figure 2).

Furthermore, it should be noted that all cases reported here have been treated with a scattering or uniform scanning system. The use of SOBP fields will significantly lessen as new centers use exclusively PBS delivery systems. There will be differences in dose distributions delivered by these distinct delivery technologies, SOBP and PBS. The characteristic avoidance of apertures in PBS in many cases will produce a larger lateral and distal penumbral volume. The PBS planning approach will change dose at the margins through optimization, to ensure target coverage. Finally, in PBS approaches the underlying LET distribution will also change as compared to SOBP, with a possible impact on RBE.

Uncertainties

Proton radiotherapy uses the proton pristine Bragg peak to achieve dose distributions that are characterized for a single field by (1) the absence of dose beyond the Bragg peak distal fall-off penetration, (2) an intrinsic sharper penumbra compared to X-ray (at least below 160 mm range), and for multiple fields by (3) the sharp reduction in integral penumbral dose that, in X-rays, is the consequence of the overlap of entrance and exit dose regions of many beams. Thus, proton radiotherapy dose distributions significantly reduce the integral normal tissue "dose bath" and allow for sharper dose fall-off.

The uncertainties in proton radiotherapy are similar to those in X-ray treatment, but also include additional factors such as uncertainties in proton penetration depth in tissue and the very strong effects of in-patient heterogeneities.[68] Proton penetration depth uncertainty, in particular, is a specific limitation of ion therapy and a consequence of the lack of accurate stopping power data (the change in proton range or energy per unit distance).

In clinical practice for SOBP fields, target coverage is preserved with (1) a longitudinal range margin along the proton beam axis that compensates for CT-Hounsfield number variability and conversion to tissue relative proton stopping power, (2) a lateral margin between the target and the aperture edge to achieve penumbral dose build-up that also includes a margin for setup uncertainties, and (3) through appropriate design of the range-

compensators ('smearing'), that ensures that setup variations (and thus variations in the imaging defined depth to the distal target surface) preserve distal coverage. Further details can be found in Moyers *et al.* [69] and Paganetti *et al.* [49].

Clinical Use of RBE in Treatment Planning

The biological dose is calculated by using the physical dose and assuming a constant RBE conversion factor of 1.1. For example, a prescription of 59 Gy (RBE) requires a physical dose calibration to 53.6 Gy. As described in previous sections, the use of a constant RBE throughout is a simplification and not the originally intended use of RBE that was to accommodate target dose prescriptions.[70].

As noted by Paganetti [49, 71, 72], the RBE in a protocol should be specified at known dose limits (from photon radiation therapy practice); ideally, one should not change dose limits to accommodate an RBE of 1.1 due to concern for possible complications. For example, MGH lowers the prescription dose to accommodate a lower brainstem dose given concern about brainstem tolerance. Instead, one might state that the brainstem dose tolerance remains 59 Gy (RBE) as in photon therapy, but that the RBE is 1.2 as demonstrated below (Table 1).

To illustrate the effect of variable RBE, we consider our specific issue: Is there an increase in brainstem complication when comparing proton and photon doses that assume an RBE = 1.1? We note in Figure 3 consequences of RBE variability between target and brainstem.

Treatment Plan Examples from Three Pediatric Proton Treatment Centers

Treatment Setup Imaging

Treatment setup for posterior fossa proton therapy relies, at all three institutions, on orthogonal X-ray imaging. Treatment planning guidelines applied at the three institutions are presented in Table 1. Plan examples from the three institutions are presented in Figures 2, 4–7.

University of Florida

The UF dosimetric guidelines for organs at risk (OARs) are shown in Table 2. To meet brainstem and spinal cord constraints, field aperture reductions are used for the final treatment fractions.

Massachusetts General Hospital

MGH procedures use the following guidelines:

1.   Prescription dose of 54 Gy (RBE), with a maximum of 55.5 Gy (RBE)

2.   Spinal Cord dose less than 50.4 Gy (RBE) (i.e. 2 fractions must be given as cone-down) with a maximum dose of 52.0 Gy (RBE) at the cord / brainstem junction

3.   No hot spots, defined as points over 55.5 Gy (RBE) in the brainstem

4. PA and left/right oblique fields, at angles ~25 degrees to normal direction, treated in PA/left and PA/right on alternating days.

5. Normal tissue constraints vary based on tumor location, age, histology and additional patient and tumor characteristics but in general are similar to guidelines used by University of Florida (Table 2)

M D Anderson Cancer Center

General guidelines with no rigid templates are used for treatment planning. Treatment plans are done based on tumor location and size. An example treatment plan is shown in Figure 7.

The main objective is to avoid distal proton range fall-off and overlap of more than one beam in the brainstem or spinal cord. If, due to non-brainstem OAR doses or high dose conformality, a PA-beam that ranges into the brainstem provides the best solution, then it may be given a lower weight. The non-PA beams are "lateral-like" at strategic oblique angles using couch and gantry rotation as required by the patient and tumor geometry. As an alternative to a PA beam, a superior oblique vertex beam that parallels the angle of the brainstem may be considered to improve high dose conformality. This approach requires excellent set-up to reproduce the head tilt and robust evaluation to predict dose variability due to positional uncertainties.

The primary plan delivers 50.4 Gy with a 3.6 Gy cone down to meet the brainstem and spinal cord dose constraints. The boost plan may consist of only two lateral-like beams. All fields are treated daily. Normal tissue constraints are given in Table 3.

Conclusions and Next Steps

The biology of brainstem injury is complex and yet requires prospective assessment to understand the intricacies involving qualitative and quantitative imaging changes, clinical symptoms and signs, and correlations of proton dose, delivery, and biological dose effect. Critical vetting of radiation planning, dosimetry, and treatment techniques should be pursued for both protons and photons, as recently reported by Indelicato[40]. It is clear that the RBE of proton beams in some areas of a spread-out Bragg peak is higher than 1.1, and that current treatment planning software does not fully account for this. There is consensus amongst those participating in the Workshop that differences in LET (and, by implication, RBE) when treating posterior fossa tumors anatomically adjacent to the brainstem contribute to brainstem injury. It appears to be that the standard 1.1 correction of physical dose for biologic effect understates the physical equivalence of proton dose in the end-of-beam and lateral margins of the proton beam. The finding of imaging changes with or without clinical signs of brainstem dysfunction is evidence of a normal tissue effect comparing protons to photons, one that appears related to differences in biological dose equivalence in regions of higher LET. Evidence has been presented here and documented independently in the literature by two of the major referral centers participating in the Workshop suggesting brainstem sensitivity to proton irradiation when the standard RBE corrected dose exceeds the "conventional" brainstem tolerance of 54 Gy photon equivalent. The two noted institutions have documented reductions in the frequency of brainstem injury when the

proton dose is conventionally adjusted (for RBE), and when treatment planning constraints and proton delivery modify proton trajectories to limit brainstem exposure to the distal or lateral aspects of the SOBP (where LET and RBE are greater than the standard correction of 1.1). We need to begin to optimize treatment planning around LET, but must tread cautiously in further understanding changes in LET and, ultimately, RBE. LET optimization is a less complex problem to address and therefore will likely be an early step in the process, optimizing plans to ensure LET hot spots remain outside normal tissues. RBE optimization might eventually follow [74], but is currently challenging as the majority of experimental data are based on cell survival *in vitro*. RBE values *in vivo*, particularly for normal tissues, might never be known to sufficient accuracy to render RBE optimization safe

The presented methodologies from three centers show robust, clinically-proven approaches for proton irradiation that were developed to decrease risk to the brainstem when treating posterior fossa tumors. The current techniques outlined herein require dose and/or volume constraints to the brainstem, including reductions in prescribed dose to the tumor and targeting that limits the CTV extent within the brainstem, thereby reducing incident physical dose to the underlying brainstem when delivering a high local dose for posterior fossa neoplasms.

Research examining biologic dosimetry and planning is important to the field moving forward, and parallel radiobiological research needs to take place to assess patient-specific biomarkers and interventions that may help prevent and detect radiation injury. A first step in this process was the Workshop as documented here. The next step has been the proposed modifications of COG's ependymoma treatment guidelines for ACNS0831, reducing the dose constraints and volume requirements for proton therapy toward levels suggested in the experience of the major reporting institutions in this paper. Several investigators have questioned whether parallel changes in photon constraints are warranted, as well. Given the sensitivities inherent to high-dose proton irradiation that includes the brainstem, it seems wise to introduce specific constraints on proton doses to the dorsal brainstem in the cooperative group setting; it is not intended to be a rigid precedent for proton therapy guidelines in the future. One looks toward the development of hypothesis driven research projects within COG and at institutions that can move the field forward, while noting that vendors are beginning to examine biologic treatment dosimetry and plan optimization that is associated with risks to normal tissues.

Individuals in the field have been exceedingly responsive, evidenced by the proliferation of reports addressing these complex issues and by this Workshop that gathered disparate healthcare professionals and scientists to examine the evidence in a collaborative, unbiased, open minded fashion. To move forward requires acceptance of the fact that (a) physical dose does not necessarily reflect biologically effective dose in particle therapy, and (b) we have not developed our treatment algorithms to adequately reflect normal tissue tolerance in photon or proton therapy. Thus, the biologically correct calculation of dose in proton therapy may exceed normal tissue tolerances. Solutions to this include more biologic research, evolving radiation planning approaches, and software development to show biologic dose visually in a format that is easier to understand and analyze.[73] As well, the field needs to monitor limited-term morbidities, especially as we introduce IMPT routinely in managing

pediatric brain tumors. Inter-patient variability might be substantial, affecting both proton and photon treatments and thus making it difficult to identify effects solely caused by elevated RBE values.

References

1. Flanz J, Bortfeld T. Evolution of technology to optimize the delivery of proton therapy: The third generation. Semin Radiat Oncol. 2013; 23:142–148. [PubMed: 23473692]

2. Oeffinger KC, Mertens AC, Sklar CA, Kawashima T, Hudson MM, Meadows AT, Friedman DL, Marina N, Hobbie W, Kadan-Lottick NS, Schwartz CL, Leisenring W, Robison LL, Childhood Cancer Survivor S. Chronic health conditions in adult survivors of childhood cancer. N Engl J Med. 2006; 355:1572–1582. [PubMed: 17035650]

3. Palm A, Johansson KA. A review of the impact of photon and proton external beam radiotherapy treatment modalities on the dose distribution in field and out-of-field; implications for the long-term morbidity of cancer survivors. Acta Oncol. 2007; 46:462–473. [PubMed: 17497313]

4. Suit H, Goldberg S, Niemierko A, Trofimov A, Adams J, Paganetti H, Chen GT, Bortfeld T, Rosenthal S, Loeffler J, Delaney T. Proton beams to replace photon beams in radical dose treatments. Acta Oncol. 2003; 42:800–808. [PubMed: 14968940]

5. Merchant TE. Cllinical controversies: Pediatric tumors. Semin Radiat Oncol. 2012; 23:97–108.

6. (ASTRO) ASfRO. Book Proton beam therapy model policy. American Soceiety for Radiation Oncology; 2017. Proton beam therapy model policy. Editor, editor^editors

7. Indelicato DJ, Flampouri S, Rotondo RL, Bradley JA, Morris CG, Aldana PR, Sandler E, Mendenhall NP. Incidence and dosimetric parameters of pediatric brainstem toxicity following proton therapy. Acta Oncol. 2014; 53:1298–1304. [PubMed: 25279957]

8. Grant SR, Grosshans DR, Bilton SD, Garcia JA, Amin M, Chambers MS, McGovern SL, McAleer MF, Morrison WH, Huh WW, Kupferman ME, Mahajan A. Proton versus conventional radiotherapy for pediatric salivary gland tumors: Acute toxicity and dosimetric characteristics. Radiother Oncol. 2015; 116:309–315. [PubMed: 26232128]

9. Lee CT, Bilton SD, Famiglietti RM, Riley BA, Mahajan A, Chang EL, Maor MH, Woo SY, Cox JD, Smith AR. Treatment planning with protons for pediatric retinoblastoma, medulloblastoma, and pelvic sarcoma: How do protons compare with other conformal techniques? Int J Radiat Oncol Biol Phys. 2005; 63:362–372. [PubMed: 16168831]

10. Boehling NS, Grosshans DR, Bluett JB, Palmer MT, Song X, Amos RA, Sahoo N, Meyer JJ, Mahajan A, Woo SY. Dosimetric comparison of three-dimensional conformal proton radiotherapy, intensity-modulated proton therapy, and intensity-modulated radiotherapy for treatment of pediatric craniopharyngiomas. Int J Radiat Oncol Biol Phys. 2012; 82:643–652. [PubMed: 21277111]

11. Moeller BJ, Chintagumpala M, Philip JJ, Grosshans DR, McAleer MF, Woo SY, Gidley PW, Vats TS, Mahajan A. Low early ototoxicity rates for pediatric medulloblastoma patients treated with proton radiotherapy. Radiat Oncol. 2011; 6:58. [PubMed: 21635776]

12. Widesott L, Pierelli A, Fiorino C, Lomax AJ, Amichetti M, Cozzarini C, Soukup M, Schneider R, Hug E, Di Muzio N, Calandrino R, Schwarz M. Helical tomotherapy vs. Intensity-modulated proton therapy for whole pelvis irradiation in high-risk prostate cancer patients: Dosimetric, normal tissue complication probability, and generalized equivalent uniform dose analysis. Int J Radiat Oncol Biol Phys. 2011; 80:1589–1600. [PubMed: 21167651]

13. MacDonald SM, Safai S, Trofimov A, Wolfgang J, Fullerton B, Yeap BY, Bortfeld T, Tarbell NJ, Yock T. Proton radiotherapy for childhood ependymoma: Initial clinical outcomes and dose comparisons. Int J Radiat Oncol Biol Phys. 2008; 71:979–986. [PubMed: 18325681]

14. Eaton BR, Esiashvili N, Kim S, Weyman EA, Thornton LT, Mazewski C, MacDonald T, Ebb D, MacDonald SM, Tarbell NJ, Yock TI. Clinical outcomes among children with standard-risk medulloblastoma treated with proton and photon radiation therapy: A comparison of disease control and overall survival. Int J Radiat Oncol Biol Phys. 2016; 94:133–138. [PubMed: 26700707]

15. Hall P, Adami HO, Trichopoulos D, Pedersen NL, Lagiou P, Ekbom A, Ingvar M, Lundell M, Granath F. Effect of low doses of ionising radiation in infancy on cognitive function in adulthood: Swedish population based cohort study. BMJ. 2004; 328:19. [PubMed: 14703539]

16. Pulsifer MB, Sethi RV, Kuhlthau KA, MacDonald SM, Tarbell NJ, Yock TI. Early cognitive outcomes following proton radiation in pediatric patients with brain and central nervous system tumors. Int J Radiat Oncol Biol Phys. 2015; 93:400–407. [PubMed: 26254679]

17. Greenberger BA, Pulsifer MB, Ebb DH, MacDonald SM, Jones RM, Butler WE, Huang MS, Marcus KJ, Oberg JA, Tarbell NJ, Yock TI. Clinical outcomes and late endocrine, neurocognitive, and visual profiles of proton radiation for pediatric low-grade gliomas. Int J Radiat Oncol Biol Phys. 2014; 89:1060–1068. [PubMed: 25035209]

18. Yock TI, Yeap BY, Ebb DH, Weyman E, Eaton BR, Sherry NA, Jones RM, MacDonald SM, Pulsifer MB, Lavally B, Abrams AN, Huang MS, Marcus KJ, Tarbell NJ. Long-term toxic effects of proton radiotherapy for paediatric medulloblastoma: A phase 2 single-arm study. Lancet Oncol. 2016; 17:287–298. [PubMed: 26830377]

19. Kahalley LS, Ris MD, Grosshans DR, Okcu MF, Paulino AC, Chintagumpala M, Moore BD, Guffey D, Minard CG, Stancel HH, Mahajan A. Comparing intelligence quotient change after treatment with proton versus photon radiation therapy for pediatric brain tumors. J Clin Oncol. 2016; 34:1043–1049. [PubMed: 26811522]

20. Chung CS, Yock TI, Nelson K, Xu Y, Keating NL, Tarbell NJ. Incidence of second malignancies among patients treated with proton versus photon radiation. Int J Radiat Oncol Biol Phys. 2013; 87:46–52. [PubMed: 23778197]

21. Paganetti H, Athar BS, Moteabbed M, J AA, Schneider U, Yock TI. Assessment of radiation-induced second cancer risks in proton therapy and imrt for organs inside the primary radiation field. Phys Med Biol. 2012; 57:6047–6061. [PubMed: 22968191]

22. Sethi RV, Shih HA, Yeap BY, Mouw KW, Petersen R, Kim DY, Munzenrider JE, Grabowski E, Rodriguez-Galindo C, Yock TI, Tarbell NJ, Marcus KJ, Mukai S, MacDonald SM. Second nonocular tumors among survivors of retinoblastoma treated with contemporary photon and proton radiotherapy. Cancer. 2014; 120:126–133. [PubMed: 24122173]

23. Bekelman JE, Schultheiss T, Berrington De Gonzalez A. Subsequent malignancies after photon versus proton radiation therapy. Int J Radiat Oncol Biol Phys. 2013; 87:10–12. [PubMed: 23810521]

24. Yock TI, Bhat S, Szymonifka J, Yeap BY, Delahaye J, Donaldson SS, MacDonald SM, Pulsifer MB, Hill KS, DeLaney TF, Ebb D, Huang M, Tarbell NJ, Fisher PG, Kuhlthau KA. Quality of life outcomes in proton and photon treated pediatric brain tumor survivors. Radiother Oncol. 2014; 113:89–94. [PubMed: 25304720]

25. Kralik SF, Ho CY, Finke W, Buchsbaum JC, Haskins CP, Shih CS. Radiation necrosis in pediatric patients with brain tumors treated with proton radiotherapy. AJNR Am J Neuroradiol. 2015; 36:1572–1578. [PubMed: 26138138]

26. Gunther JR, Sato M, Chintagumpala M, Ketonen L, Jones JY, Allen PK, Paulino AC, Okcu MF, Su JM, Weinberg J, Boehling NS, Khatua S, Adesina A, Dauser R, Whitehead WE, Mahajan A. Imaging changes in pediatric intracranial ependymoma patients treated with proton beam radiation therapy compared to intensity modulated radiation therapy. Int J Radiat Oncol Biol Phys. 2015; 93:54–63. [PubMed: 26279024]

27. Yock TI, Constine LS, Mahajan A. Protons, the brainstem, and toxicity: Ingredients for an emerging dialectic. Acta Oncol. 2014; 53:1279–1282. [PubMed: 25327262]

28. Sabin ND, Merchant TE, Harreld JH, Patay Z, Klimo P Jr, Qaddoumi I, Armstrong GT, Wright K, Gray J, Indelicato DJ, Gajjar A. Imaging changes in very young children with brain tumors treated with proton therapy and chemotherapy. AJNR Am J Neuroradiol. 2013; 34:446–450. [PubMed: 22821924]

29. Jones B, Wilson P, Nagano A, Fenwick J, McKenna G. Dilemmas concerning dose distribution and the influence of relative biological effect in proton beam therapy of medulloblastoma. Br J Radiol. 2012; 85:e912–918. [PubMed: 22553304]

30. MacDonald SM, Laack NN, Terezakis S. Humbling advances in technology: Protons, brainstem necrosis, and the self-driving car. Int J Radiat Oncol Biol Phys. 2017; 97:216–219. [PubMed: 28068228]

31. Woodward WA, Amos RA. Proton radiation biology considerations for radiation oncologists. Int J Radiat Oncol Biol Phys. 2016; 95:59–61. [PubMed: 27084628]

32. Underwood T, Paganetti H. Variable proton relative biological effectiveness: How do we move forward? Int J Radiat Oncol Biol Phys. 2016; 95:56–58. [PubMed: 27084627]

33. Macdonald SM, Sethi R, Lavally B, Yeap BY, Marcus KJ, Caruso P, Pulsifer M, Huang M, Ebb D, Tarbell NJ, Yock TI. Proton radiotherapy for pediatric central nervous system ependymoma: Clinical outcomes for 70 patients. Neuro Oncol. 2013; 15:1552–1559. [PubMed: 24101739]

34. Giantsoudi D, Sethi RV, Yeap BY, Eaton BR, Ebb DH, Caruso PA, Rapalino O, Chen YL, Adams JA, Yock TI, Tarbell NJ, Paganetti H, MacDonald SM. Incidence of cns injury for a cohort of 111 patients treated with proton therapy for medulloblastoma: Let and rbe associations for areas of injury. Int J Radiat Oncol Biol Phys. 2016; 95:287–296. [PubMed: 26691786]

35. Ares C, Albertini F, Frei-Welte M, Bolsi A, Grotzer MA, Goitein G, Weber DC. Pencil beam scanning proton therapy for pediatric intracranial ependymoma. J Neurooncol. 2016; 128:137–145. [PubMed: 26945580]

36. Merchant TE, Li C, Xiong X, Kun LE, Boop FA, Sanford RA. Conformal radiotherapy after surgery for paediatric ependymoma: A prospective study. Lancet Oncol. 2009; 10:258–266. [PubMed: 19274783]

37. Murphy ES, Merchant TE, Wu S, Xiong X, Lukose R, Wright KD, Qaddoumi I, Armstrong GT, Broniscer A, Gajjar A. Necrosis after craniospinal irradiation: Results from a prospective series of children with central nervous system embryonal tumors. Int J Radiat Oncol Biol Phys. 2012; 83:e655–660. [PubMed: 22768993]

38. Merchant TE, Chitti RM, Li C, Xiong X, Sanford RA, Khan RB. Factors associated with neurological recovery of brainstem function following postoperative conformal radiation therapy for infratentorial ependymoma. Int J Radiat Oncol Biol Phys. 2010; 76:496–503. [PubMed: 19464817]

39. Nanda RH, Ganju RG, Schreibmann E, Chen Z, Zhang C, Jegadeesh N, Cassidy R, Deng C, Eaton BR, Esiashvili N. Correlation of acute and late brainstem toxicities with dose-volume data for pediatric patients with posterior fossa malignancies. Int J Radiat Oncol Biol Phys. 2017; 98:360–366. [PubMed: 28463155]

40. Indelicato, DJ., Bradley, JA., Rotondo, RL., Flampouri, S., Nanda, RH., Logie, N., Morris, CG., Mendenhall, NP. Oral presentation 11. Paediatric Radiation Oncology Society Congress; New York, NY: 2017.

41. Hua C, Merchant TE, Gajjar A, Broniscer A, Zhang Y, Li Y, Glenn GR, Kun LE, Ogg RJ. Brain tumor therapy-induced changes in normal-appearing brainstem measured with longitudinal diffusion tensor imaging. Int J Radiat Oncol Biol Phys. 2012; 82:2047–2054. [PubMed: 21664060]

42. Lui YW, Law M, Chacko-Mathew J, Babb JS, Tuvia K, Allen JC, Zagzag D, Johnson G. Brainstem corticospinal tract diffusion tensor imaging in patients with primary posterior fossa neoplasms stratified by tumor type: A study of association with motor weakness and outcome. Neurosurgery. 2007; 61:1199–1207. discussion 1207-1198. [PubMed: 18162899]

43. Wang S, Wu EX, Qiu D, Leung LH, Lau HF, Khong PL. Longitudinal diffusion tensor magnetic resonance imaging study of radiation-induced white matter damage in a rat model. Cancer Res. 2009; 69:1190–1198. [PubMed: 19155304]

44. Chan KC, Khong PL, Cheung MM, Wang S, Cai KX, Wu EX. Mri of late microstructural and metabolic alterations in radiation-induced brain injuries. J Magn Reson Imaging. 2009; 29:1013–1020. [PubMed: 19388094]

45. Patay Z, DeSain LA, Hwang SN, Coan A, Li Y, Ellison DW. Mr imaging characteristics of wingless-type-subgroup pediatric medulloblastoma. AJNR Am J Neuroradiol. 2015; 36:2386–2393. [PubMed: 26338912]

46. Fouladi M, Chintagumpala M, Laningham FH, Ashley D, Kellie SJ, Langston JW, McCluggage CW, Woo S, Kocak M, Krull K, Kun LE, Mulhern RK, Gajjar A. White matter lesions detected by magnetic resonance imaging after radiotherapy and high-dose chemotherapy in children with medulloblastoma or primitive neuroectodermal tumor. J Clin Oncol. 2004; 22:4551–4560. [PubMed: 15542806]

47. Uh J, Merchant TE, Li Y, Feng T, Gajjar A, Ogg RJ, Hua C. Differences in brainstem fiber tract response to radiation: A longitudinal diffusion tensor imaging study. Int J Radiat Oncol Biol Phys. 2013; 86:292–297. [PubMed: 23474114]

48. Peeler CR, Mirkovic D, Titt U, Blanchard P, Gunther JR, Mahajan A, Mohan R, Grosshans DR. Clinical evidence of variable proton biological effectiveness in pediatric patients treated for ependymoma. Radiother Oncol. 2016; 121:395–401. [PubMed: 27863964]

49. Paganetti H, Niemierko A, Ancukiewicz M, Gerweck LE, Goitein M, Loeffler JS, Suit HD. Relative biological effectiveness (rbe) values for proton beam therapy. Int J Radiat Oncol Biol Phys. 2002; 53:407–421. [PubMed: 12023146]

50. Paganetti H. Relative biological effectiveness (rbe) values for proton beam therapy. Variations as a function of biological endpoint, dose, and linear energy transfer. Physics in Medicine and Biology. 2014; 59:R419–R472. [PubMed: 25361443]

51. Goodhead DT, Thacker J, Cox R. Effects of radiations of different qualities on cells: Molecular mechanisms of damage and repair. International Journal of Radiation Biology. 1993; 63:543–556. [PubMed: 8099101]

52. Pastwa E, Neumann RD, Mezhevaya K, Winters TA. Repair of radiation-induced DNA double-strand breaks is dependent upon radiation quality and the structural complexity of double-strand breaks. Radiat Res. 2003; 159:251–261. [PubMed: 12537531]

53. McNamara AL, Schuemann J, Paganetti H. A phenomenological relative biological effectiveness (rbe) model for proton therapy based on all published in vitro cell survival data. Phys Med Biol. 2015; 60:8399–8416. [PubMed: 26459756]

54. Carabe A, Espana S, Grassberger C, Paganetti H. Clinical consequences of relative biological effectiveness variations in proton radiotherapy of the prostate, brain and liver. Physics in Medicine and Biology. 2013; 58:2103–2117. [PubMed: 23470339]

55. Giantsoudi D, Adams J, MacDonald SM, Paganetti H. Proton treatment techniques for posterior fossa tumors: Consequences for linear energy transfer and dose-volume parameters for the brainstem and organs at risk. Int J Radiat Oncol Biol Phys. 2017; 97:401–410. [PubMed: 27986346]

56. Polster L, Schuemann J, Rinaldi I, Burigo L, McNamara AL, Stewart RD, Attili A, Carlson DJ, Sato T, Ramos Mendez J, Faddegon B, Perl J, Paganetti H. Extension of topas for the simulation of proton radiation effects considering molecular and cellular endpoints. Phys Med Biol. 2015; 60:5053–5070. [PubMed: 26061666]

57. Giantsoudi D, Grassberger C, Craft D, Niemierko A, Trofimov A, Paganetti H. Linear energy transfer-guided optimization in intensity modulated proton therapy: Feasibility study and clinical potential. Int J Radiat Oncol Biol Phys. 2013; 87:216–222. [PubMed: 23790771]

58. Grassberger C, Trofimov A, Lomax A, Paganetti H. Variations in linear energy transfer within clinical proton therapy fields and the potential for biological treatment planning. Int J Radiat Oncol Biol Phys. 2011; 80:1559–1566. [PubMed: 21163588]

59. Bassler N, Toftegaard J, Luhr A, Sorensen BS, Scifoni E, Kramer M, Jakel O, Mortensen LS, Overgaard J, Petersen JB. Let-painting increases tumour control probability in hypoxic tumours. Acta Oncol. 2014; 53:25–32. [PubMed: 24020629]

60. Grassberger C, Trofimov A, Lomax A, Paganetti H. Variations in linear energy transfer within clinical proton therapy fields and the potential for biological treatment planning. International Journal of Radiation Oncology, Biology, Physics. 2011; 80:1559–1566.

61. Unkelbach J, Botas P, Giantsoudi D, Gorissen B, Paganetti H. Reoptimization of intensity-modulated proton therapy plans based on linear energy transfer. International Journal of Radiation Oncology Biology Physics. 2016; 96:1097–1106.

62. Bassler N, Jakel O, Sondergaard CS, Petersen JB. Dose- and let-painting with particle therapy. Acta Oncol. 2010; 49:1170–1176. [PubMed: 20831510]

63. Fager M, Toma-Dasu I, Kirk M, Dolney D, Diffenderfer ES, Vapiwala N, Carabe A. Linear energy transfer painting with proton therapy: A means of reducing radiation doses with equivalent clinical effectiveness. Int J Radiat Oncol Biol Phys. 2015; 91:1057–1064. [PubMed: 25832696]

64. Chen RC, Gabriel PE, Kavanagh BD, McNutt TR. How will big data impact clinical decision making and precision medicine in radiation therapy? Int J Radiat Oncol Biol Phys. 2016; 95:880–884. [PubMed: 26797536]

65. Kooy HM, Rosenthal SJ, Engelsman M, Mazal A, Slopsema RL, Paganetti H, Flanz JB. The prediction of output factors for spread-out proton bragg peak fields in clinical practice. Phys Med Biol. 2005; 50:5847–5856. [PubMed: 16333159]

66. Sahoo N, Zhu XR, Arjomandy B, Ciangaru G, Lii M, Amos R, Wu R, Gillin MT. A procedure for calculation of monitor units for passively scattered proton radiotherapy beams. Med Phys. 2008; 35:5088–5097. [PubMed: 19070243]

67. Hong L, Goitein M, Bucciolini M, Comiskey R, Gottschalk B, Rosenthal S, Serago C, Urie M. A pencil beam algorithm for proton dose calculations. Phys Med Biol. 1996; 41:1305–1330. [PubMed: 8858722]

68. Urie M, Goitein M, Wagner M. Compensating for heterogeneities in proton radiation therapy. Phys Med Biol. 1984; 29:553–566. [PubMed: 6330772]

69. Moyers MF, Miller DW, Bush DA, Slater JD. Methodologies and tools for proton beam design for lung tumors. Int J Radiat Oncol Biol Phys. 2001; 49:1429–1438. [PubMed: 11286851]

70. Munzenrider JE, Austin-Seymour M, Blitzer PJ, Gentry R, Goitein M, Gragoudas ES, Johnson K, Koehler AM, McNulty P, Moulton G, et al. Proton therapy at harvard. Strahlentherapie. 1985; 161:756–763. [PubMed: 3001976]

71. Paganetti H. Significance and implementation of rbe variations in proton beam therapy. Technol Cancer Res Treat. 2003; 2:413–426. [PubMed: 14529306]

72. Paganetti H. Relative biological effectiveness (rbe) values for proton beam therapy. Variations as a function of biological endpoint, dose, and linear energy transfer. Phys Med Biol. 2014; 59:R419–472. [PubMed: 25361443]

73. Qutub MA, Klein SB, Buchsbaum JC. Rapid rbe-weighted proton radiation dosimetry risk assessment. Technol Cancer Res Treat. 2016; 15:NP1–7.
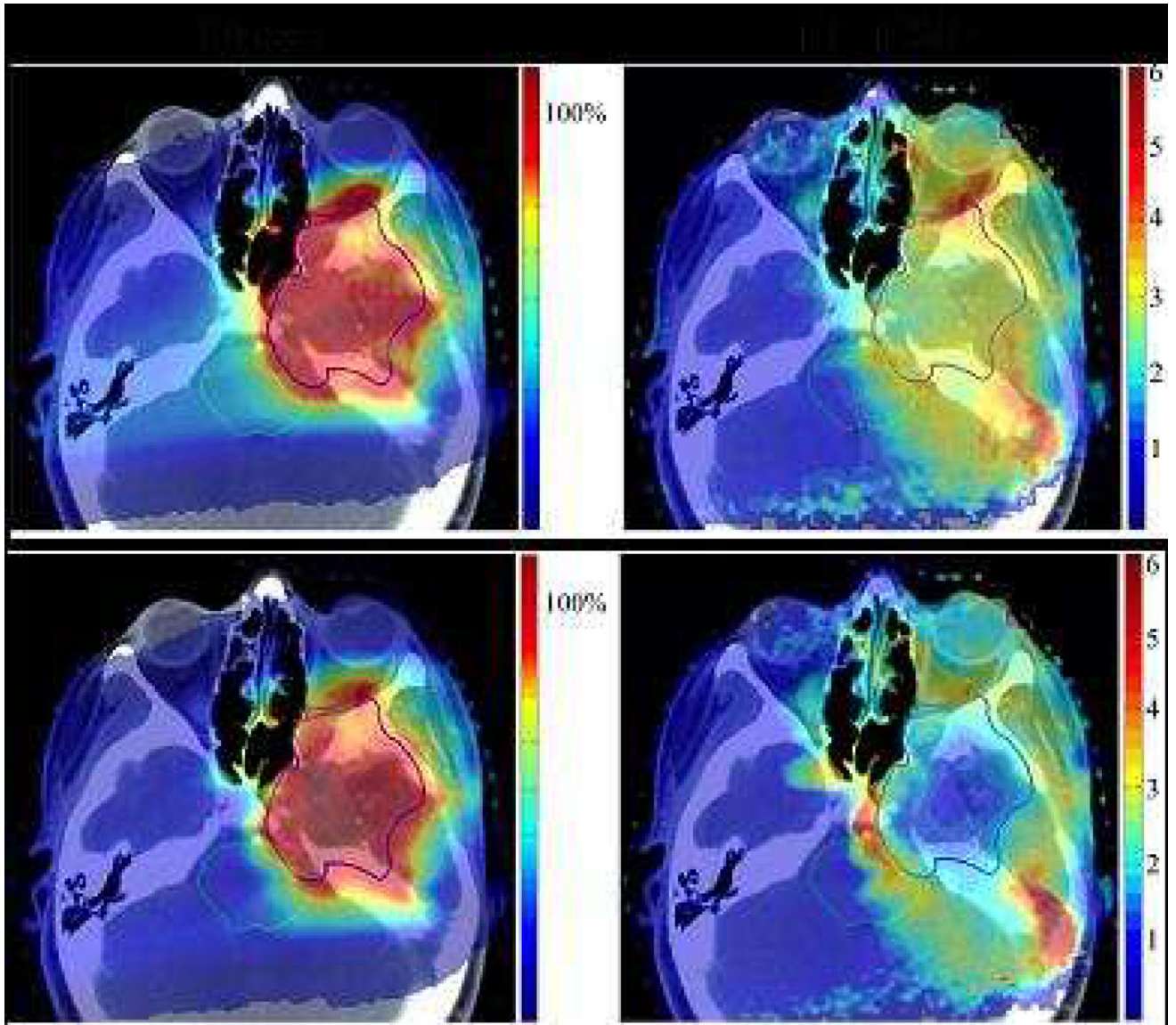
Figure 1.
Two IMPT plans that display clinically equivalent dose distributions, but different LET distributions. (Chordoma; dose in % of prescribed dose; GTV line in blue. The right column shows the mean LET$_d$ distributions in kev/μm).
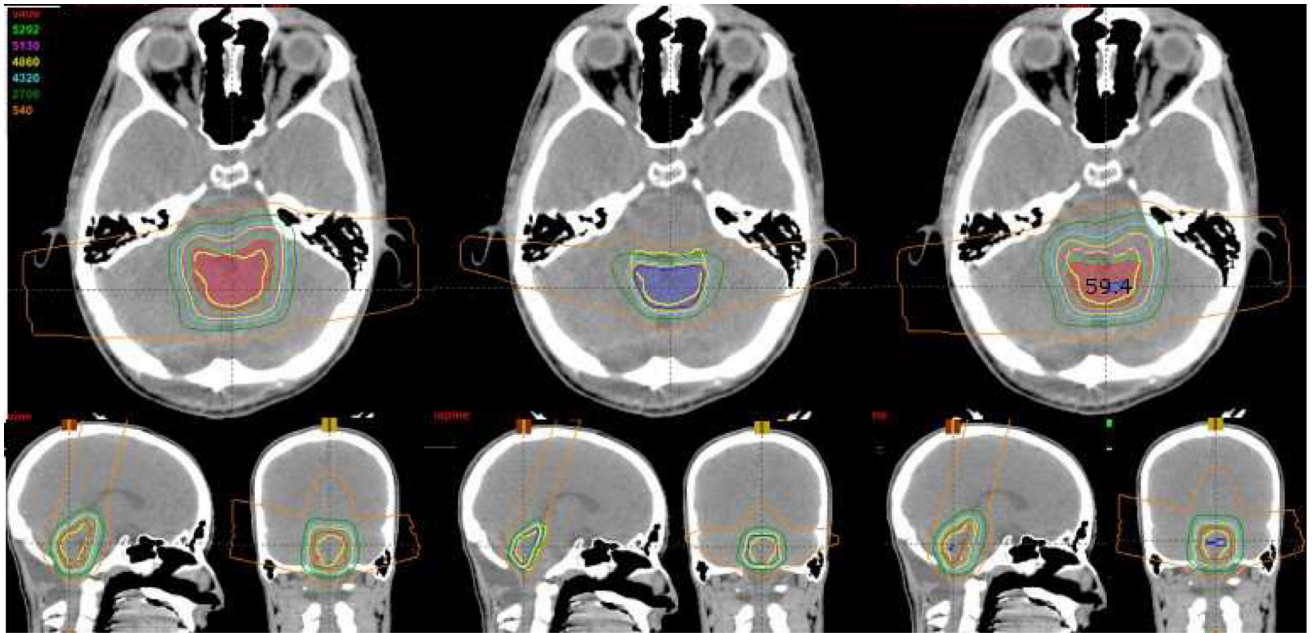
Figure 2.
University of Florida. Ependymoma proton treatment example with 59.4 CGE prescribed to the clinical target volume CTV (yellow). Left: Initial phase 54.0 CGE, (red dose-wash), priority is given on target coverage. Middle: Reduction phase 5.4 CGE (blue dose-wash), priority is given to brainstem sparing. And Right: Composite dose distribution, 59.4 CGE (red dose-wash). Target volume is depicted in yellow contour.
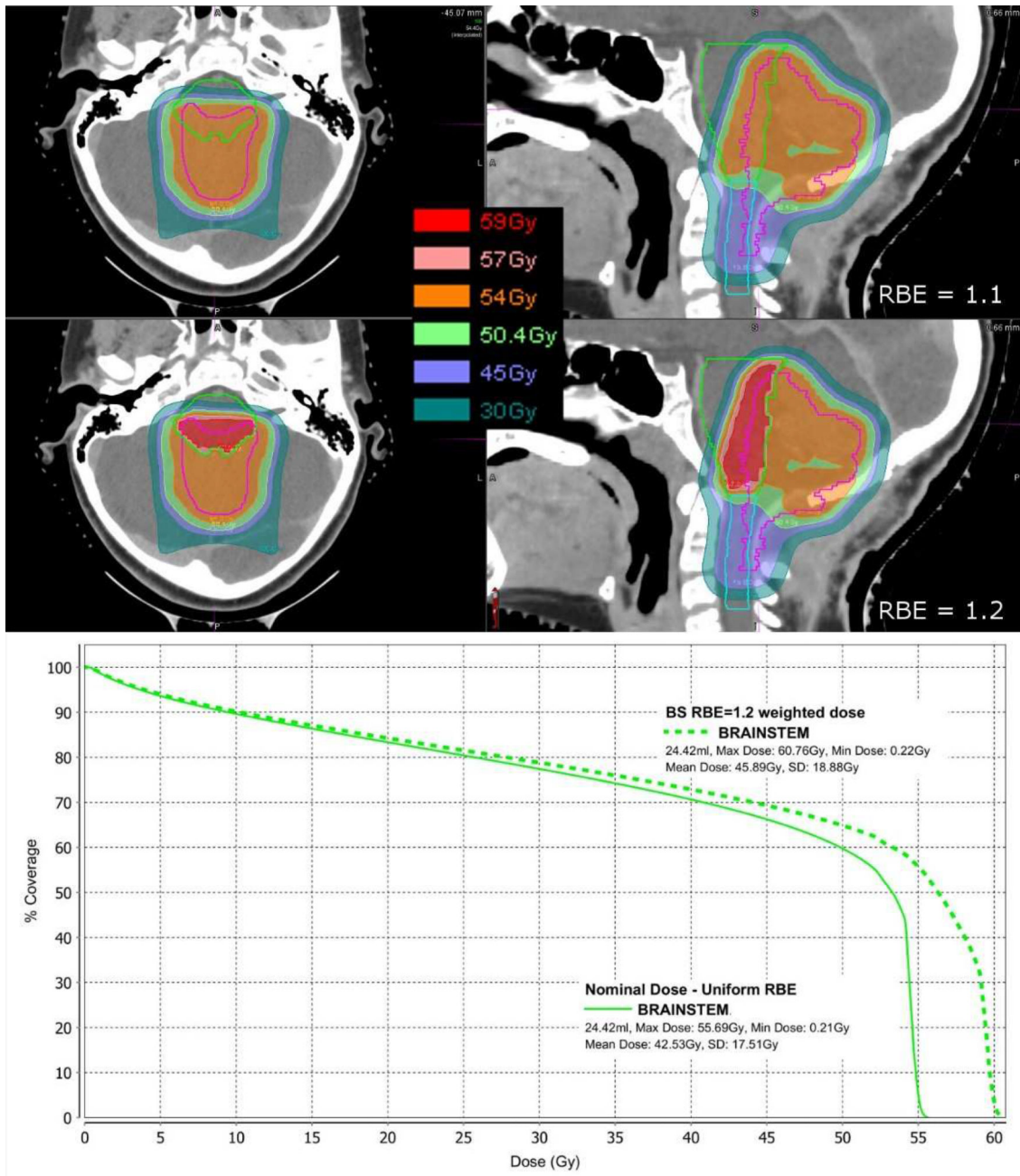
Figure 3.
Dosimetry for the MGH patient (see Fig. 5) if the brainstem RBE = 1.1 (top dosimetry panels) or 1.2 (bottom dosimetry panels) while for other tissues RBE = 1.1
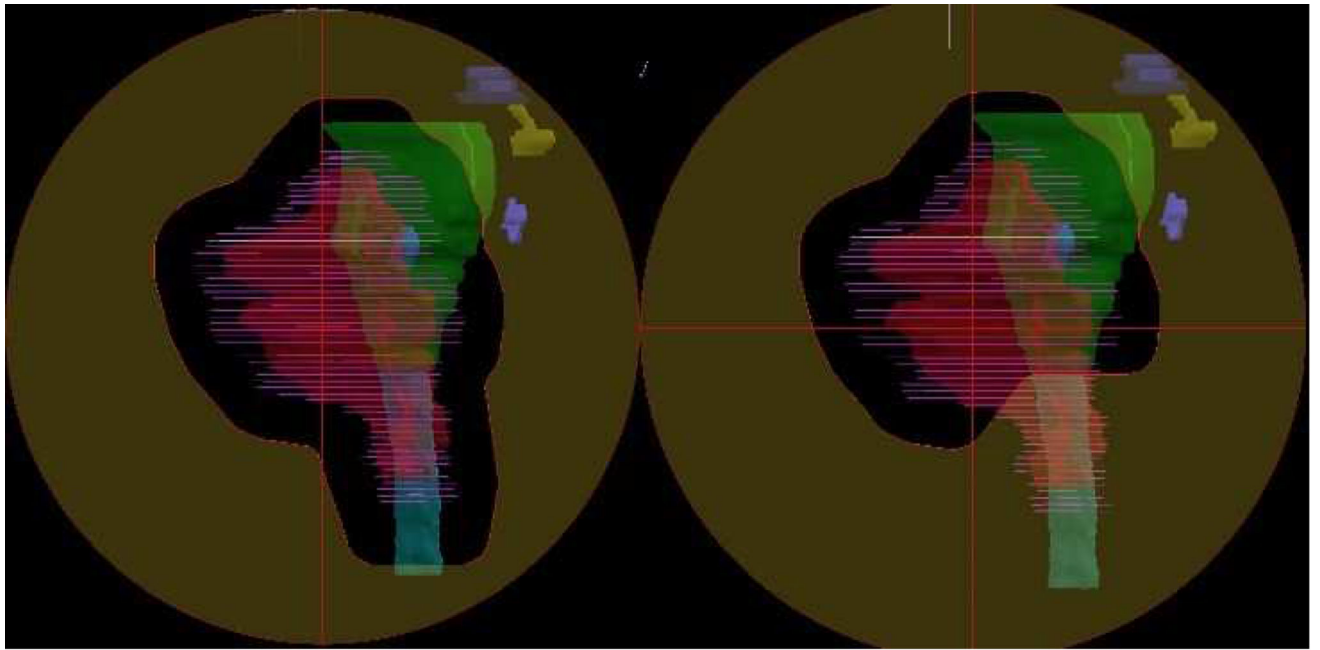
Figure 4.
MGH: Right oblique for the total CTV (purple, left) up to 50.4 and cone down (right) at the cord / brainstem junction. Also shown are the cochlea, pituitary and hypothalamus. Often, but not in this case, the aperture is tightened along the brainstem surface to reduce dose to the brainstem in the cone-down as applied in the UF treatment parameters shown in Table 2.

Figure 5.
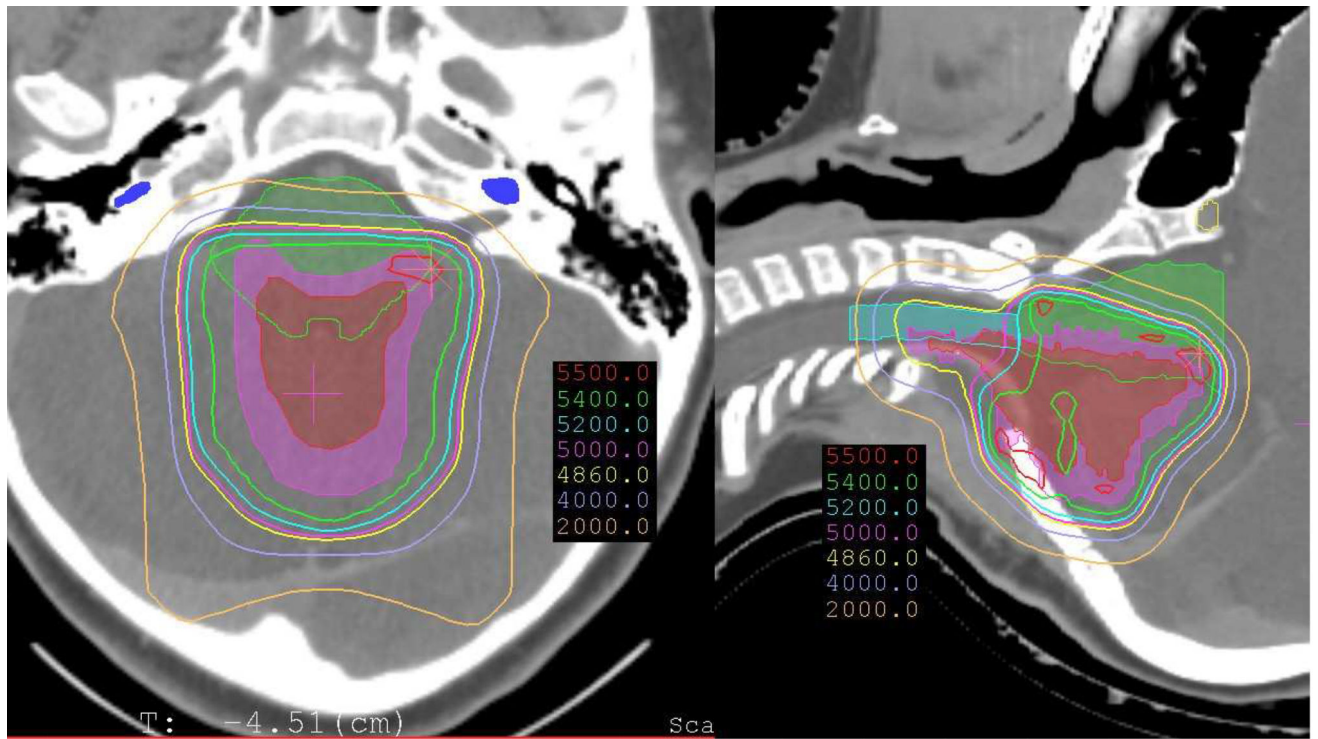MGH. Transverse and sagittal proton dose distributions. Note the 52 Gy (RBE) isodose at the cord (cyan) / brainstem (green except in GTV / CTV overlap) junctions. A few hotspots of 55 Gy (RBE) are also observed.
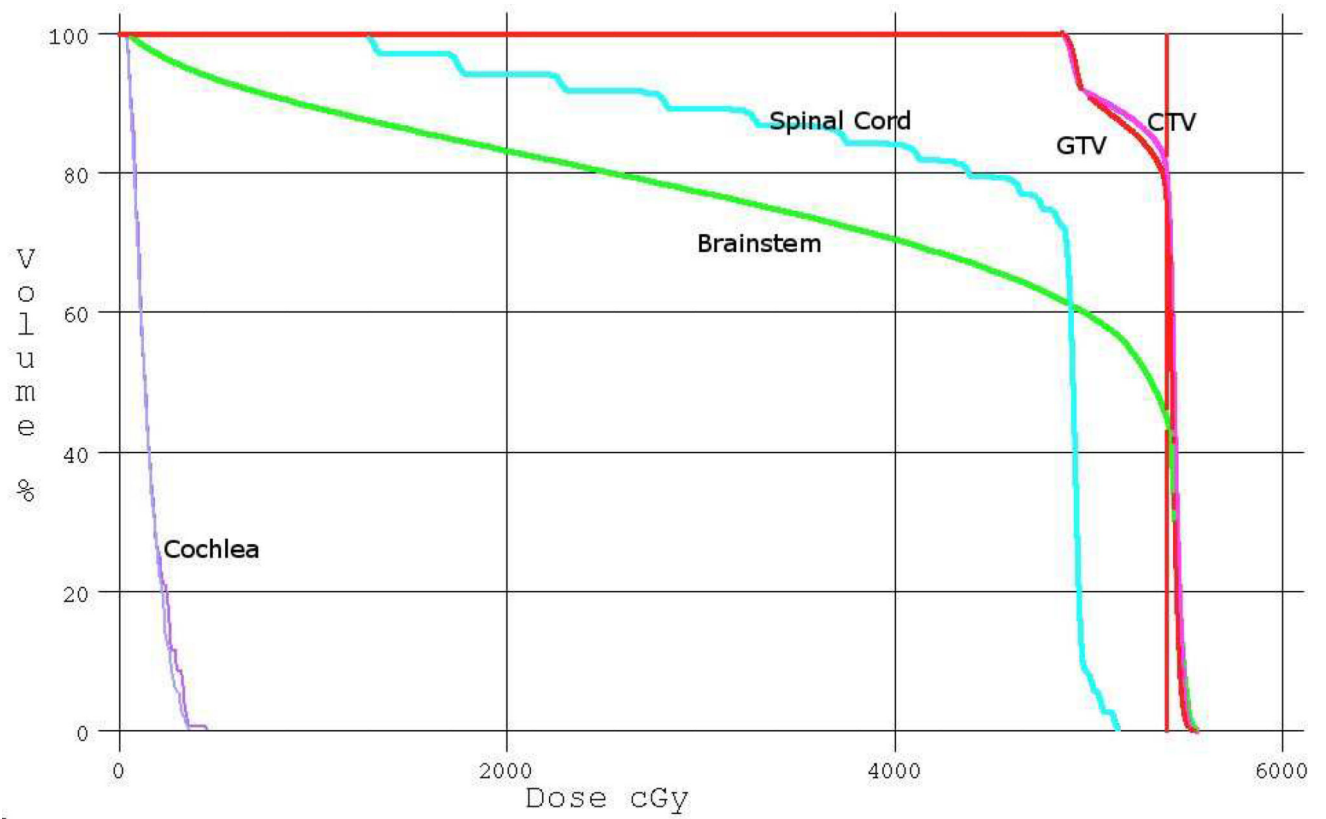
Figure 6.
MGH. DVH for the patient shown in Fig. 5. Note the GTV / CTV dose deficit dictated by
the spinal cord constraint and the sharp fall-off of dose for the targets and brainstem.

Figure 7.
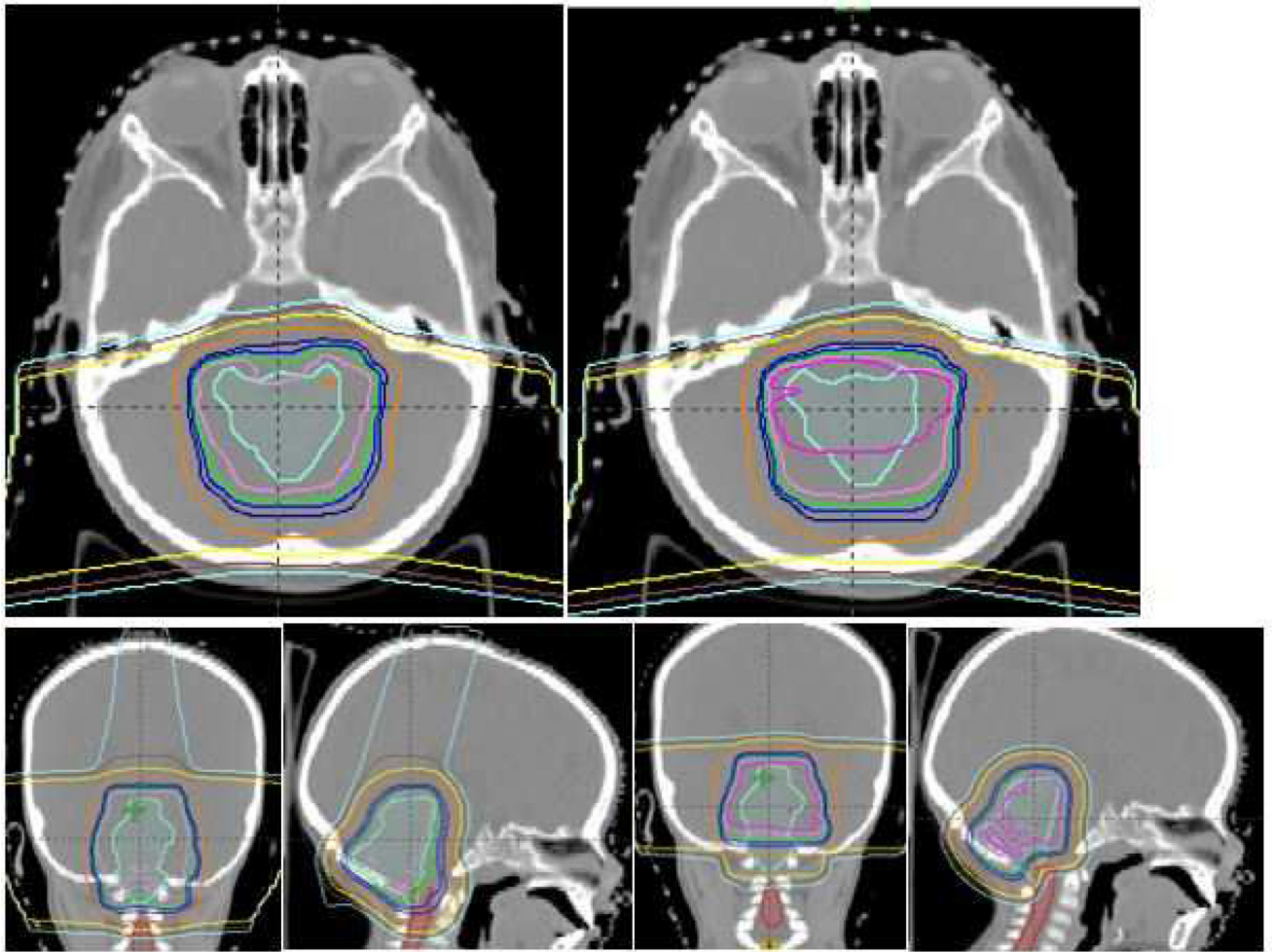MDACC:The left transverse, sagittal and coronal panels show the primary course dose using 2 posterior oblique fields and a vertex field to 50.4 Gy (RBE). The right panels show the boost of 3.6 Gy (RBE) and indicate the dose reduction to the spinal cord. Prescription dose levels, 50.4 on the left group of three images and the boost of 3.6 Gy (RBE) on the right set of three images, are in green.

Table 1

Treatment planning parameters for double scattered proton therapy delivery

	UF	MGH	MDA
PTV-CTV margin	3 mm – PTV used for lateral shaping of the collimator and for plan evaluation	No PTV, implicit in margin of CTV to aperture.	2–3 mm – used for plan evaluation
CTV volume (cc)	8–252 cc Median 39cc	2.89–302.75 cc Median 69.72 cc	12.3–218.5 cc Median: 42.25 cc
Number of Fields	3 (daily)	3 (2 per day)	2–3 daily
Approach	Most common: Posterior / Out-of-plane superior obliques	In-plane posterior and left / right posterior obliques	Most common: 2 laterals and PA. Beam angles may be modified according to specific location of the tumor
Brainstem	1 beam range-out	Multiple beams can range out but cannot range out in the same location; oblique field aperture penumbrae added to the range-out penumbra mitigate the range-out effect	1 beam range-out
Type	SOBP	SOBP	SOBP
Distal margin (mm) given as percentage of field range R plus additional increment per practice	2.5% R + 1.5 mm	3.5% R + 1 mm	3.5% R + 3 mm
Proximal margin (mm)	As distal margin	As distal margin	Based on formula, usually 3–4 mm
Aperture margin (mm)	7 mm from PTV	8 mm from CTV	7 mm from CTV with acceptance of 96% PTV coverage
Compensator smear (mm)	5 mm	3 mm and matched to 2 mm beyond the target distal surface	5 mm
Brainstem margin	Aperture tightening to "cone-down" on CTV only.	Aperture tightening near OAR to "cone-down" on CTV only.	Aperture tightening to "cone-down" on CTV only.

Brainstem constraints Doses in Gy (RBE) with RBE = 1.1

	UF		MGH	MDA	
	Goal	Max	Directive	Goal	Max
	0.1 cc	56.6	58	Max 55 Gy (RBE) if gross-total resection, 56–58 Gy (RBE) with residual. D10% not used. D50% 52.4 Gy (RBE) but often not	<20% 54	0.1cc <58
	10%	55.4	56		<50% 52	

	UF			MGH	MDA
	50%	52.4	54	achievable. Total dose typically below 59.4 Gy (RBE).	
Notes:	Patients > 3 years old with ependymoma are treated to 59.4 Gy (RBE). Infants with ependymoma who have undergone a gross total resection receive 54 Gy (RBE). All patients with medulloblastoma receive a boost to 54 Gy (RBE). No plan to exceed any max dose metric or 1 goal dose metric. Patients < 5 years old should not exceed any goal dose metric			Only patients with ependymoma gross disease get 59.4 Gy (RBE) and sometimes 57.6 Gy (RBE). Usually patients receive 54 Gy (RBE), with only small spots of 54.5 and max of 55	Effort is made to cover gross residual disease to 59.4 Gy (RBE) but brainstem tolerance is higher priority and dose will be reduced to GTV accordingly
Goals	Goal to cover CTV 100% and PTV >95%, but brainstem, chiasm, and spinal cord take priority			No hard constraints. Aim to achieve coverage similar to UF but allow lower dose coverage of CTV near important organs (including cochlea)	Goal to cover CTV 100% and PTV >95%, but brainstem and spinal cord will take priority

Table 2

The dosimetric constraints practiced at the University of Florida and applied in the sample treatment plan case, Figures 3–4. Similar guidelines individualized by patient and tumor characteristics are followed at the Massachusetts General Hospital.

Structure		DHV Point	Goal	Acceptable Range	
Target	CTV	Relative dose at 99% volume	100%		
	CTV	Relative volume at 99% dose	100%		
	GTV	Relative dose at 99% volume	100%		
	GTV	Relative volume at 99% dose	100%		
OAR					
	Brainstem	Absolute dose at 0.1 cc	<56.6 Gy	56.6	D0.1cc < 58
		Absolute dose at 50% volume	<52.4 Gy	52.4	D50% < 54
		Absolute dose at 10% volume	<55.4 Gy	55.4	D10% < 56
	Optic Chiasm	Absolute dose at 0.1 cc	<55 Gy	55	D0.1cc < 60
	Optic Nerve	Absolute dose at 0.1 cc	<55 Gy	55	D0.1cc < 60
	Cochlea	Mean absolute dose	<30 Gy	30	Dmean < 36
	Retina	Absolute dose at 0.1 cc	<50 Gy	50	D0.1cc < 55
	Lacrimal Gland	Mean absolute dose	<34 Gy	34	Dmean < 41
	Spinal Cord	Absolute dose at 1 cc	<50.4 Gy	50.4	D1cc < 52.2
		Absolute volume at 50.4 Gy	<5 cc	ALARA	
		Maximum absolute dose	<54 Gy	ALARA	
	Hippocampus Head	Mean absolute dose	<5 Gy	ALARA	
	Hippocampus Tail	Mean absolute dose	<20 Gy	ALARA	
	Hypothalamus	Mean absolute dose	<5 Gy	ALARA	
	Masticators	Relative volume at 40 Gy	<20%	ALARA	
	Mastoid	Mean absolute dose	<30 Gy	ALARA	
	Nasopharynx Posterior	Mean absolute dose	<30 Gy	ALARA	
	Brain	Relative volume at 115% dose	0%	ALARA	
	Brainstem Core	Absolute dose at 0.1 cc	<56.1 Gy	ALARA	
	Pituitary	Mean absolute dose	<30 Gy	ALARA	
	Scalp	Absolute volume at 30 Gy	<5 cc	ALARA	
	Temporal Lobe	Relative volume at 20 Gy	<10 %	ALARA	
	Circle of Willis (#)	Estimated dose	<10 Gy	ALARA	

Table 3

Normal tissue constraints applied at MD Anderson Cancer Center in clinical practice for posterior fossa targets.

Structure	Regular constraints	Other constraints (¥)
Spinal Cord	Max dose 51 Gy	V45Gy 1 cc
		V50.4Gy 1 cc
		Max dose 52 Gy
		V60Gy 0.01 cc
Brainstem:	Max dose 57 Gy	V55Gy 0.5 cc
	V54Gy 10 %	V30Gy 33%
Brain:	V30Gy 50%	
Chiasm	Max dose 54 Gy	
Cochlea (Left/Right)	Max dose 45 Gy	
	Mean dose 30 Gy	Mean dose 38 Gy
Eye (Left/Right)	Max dose 40 Gy	
	Mean dose 30 Gy	
Hippocampus (Left/Right)	D100% 9 Gy	
	Max dose 16 Gy	
Hippocampus (Left/Right)	D100% 9 Gy	
	Max dose 16 Gy	
Lacrimal Gland (Left/Right)	Mean dose 10 Gy	
Lens (Left/Right)	Max dose 5 Gy	ALARA
Mandible	Max dose 70 Gy	
Optic Nerve (Left/Right)	Max dose 54 Gy	
Parotid Gland (Left/Right)	Mean dose 10 Gy	Mean dose 15 Gy
Pituitary	Mean dose 36 Gy	
Skin	Max dose 66 Gy	
Temporal lobe	Max dose 70 Gy	ALARA
Thyroid	ALARA	

¥
Allowed constraints depending on tumor location and age